

# Biotinylated disulfide containing PEI/avidin bioconjugate shows specific enhanced transfection efficiency in HepG2 cells

Xuan Zeng, Yun-Xia Sun, Xian-Zheng Zhang\* and Ren-Xi Zhuo

Received 3rd June 2009, Accepted 2nd July 2009

First published as an Advance Article on the web 11th August 2009

DOI: 10.1039/b910831a

Targeting of non-viral gene vectors to liver cells could offer the opportunity to cure liver diseases. In this paper, disulfide-containing polyethylenimine (PEI-SS) was synthesized from low molecular weight branched PEI and cystamine bisacrylamide (CBA), and then grafted with biotin. The obtained biotinylated PEI-SS was bioconjugated with avidin *via* the biotin-avidin interaction to form a novel gene vector, biotinylated PEI-SS/avidin bioconjugate (ABP-SS). Characteristics of ABP-SS and its pDNA complexes were evaluated in terms of acid-base titration, agarose gel electrophoresis, SEM morphology observation, particle size and  $\zeta$ -potential measurements, and PEI-SS was used as the control. The acid-base titration results showed that ABP-SS exhibited comparable buffer capability to 25 kDa PEI. The results of gel electrophoresis indicated that ABP-SS was able to condense pDNA efficiently at an N/P ratio of 6 and could be degraded by reducing agent DTT. The ABP-SS/pDNA complexes had a mean particle size of  $226 \pm 40$  nm and surface charges of 25 mV. The SEM images showed that the complexes had compact structures with spherical or quadrate shapes. *In vitro* cell viability and transfection of ABP-SS and PEI-SS were compared in HepG2, 293T and H446 cells. Among the three different cell lines, compared with PEI-SS, ABP-SS exhibited much lower cytotoxicity and higher transfection efficacy in HepG2 cells due to the biocompatibility of avidin and the specific interactions between avidin and HepG2 cells. Molecular probes were used to reveal the cellular uptake of complexes, and the results demonstrated that ABP-SS contributes to more cellular uptake of complexes in HepG2 cells, which was consistent with the transfection results.

## Introduction

Gene therapy is a new form of molecular medicine to cure the inherited or acquired diseases through delivering normal genes to targeted cells and replacing the disorder genes. Nowadays, large numbers of non-viral gene vectors, including cationic liposomes and polycation, have attracted much attention due to their lower toxicity, low immune response, simple preparation and greater stability as compared with viral vectors.<sup>1</sup> Polyethylenimine (PEI) is one of the most effective non-viral gene vectors, which presents significantly high transfection capability in various cells because of the proton sponge effect which can buffer the pH value of endosome and cause the release of the complex into the cytoplasm.<sup>2</sup> However, PEI with a high molecular weight (25 kDa PEI) shows high cytotoxicity which severely limits its clinical applications. Therefore, several biodegradable PEIs and crosslinked low molecular weight PEIs have been developed to reduce the cytotoxicity.<sup>3</sup> The degradable PEI gene vectors were obtained *via* reversible disulfide bonds and it was found that the crosslinked PEI gene vector exhibited comparable transfection efficiency and lower toxicity as compared with 25 kDa PEI.<sup>4</sup>

Moreover, making the gene vector specific in distinguishing the target cells from the non-target cells will achieve remarkably enhanced transfection efficiency, reduce the required therapeutic vector doses and lower the overall toxicity to the host. In order

to provide cationic vectors with cell specificity in gene delivery, cell targeting ligands are attached to the vectors which can be recognized by specific interactions with the target cells. The ligands could be vitamins, carbohydrates, peptides, proteins or antibodies, and the choice of ligand is the key to extracellular gene delivery, cellular uptake and intracellular gene expression.<sup>5</sup> Chicken egg white avidin (66 kDa) is a tetrameric protein that binds biotin with high affinity, and the avidin-biotin system has been widely used as a linker for surface modification, biochemical techniques and tumor targeting studies.<sup>6</sup> Furthermore, avidin contains lysine, arginine, aspartic acid, glutamic acid and mannose residues, and it exhibits a remarkable accumulation in liver.<sup>7</sup>

Hepatocellular carcinoma (HCC) accounts for 80% of primary liver tumors in adults, it has a poor 5-year survival rate of about 7% despite treatments.<sup>8</sup> Conventional treatments such as liver transplantation can only be applied in the management of the early HCC patients.<sup>9</sup> Therefore, gene therapy is considered as a potential diagnostic and therapeutic approach, which provides possibilities for the delivery of gene into hepatic tumors, increasing the effective dose and minimizing potential side effects. Significant progress in HCC gene therapy has been made during recent years, attributed to the development of effective gene transfer vectors.<sup>10</sup>

In this study, avidin was bound with the biotinylated PEI-SS (BP-SS) through the biotin-avidin interaction to form a novel vector, biotinylated PEI-SS/avidin bioconjugate (ABP-SS). Characteristics of ABP-SS and its pDNA complexes were evaluated by acid-base titration, agarose gel electrophoresis, SEM morphology

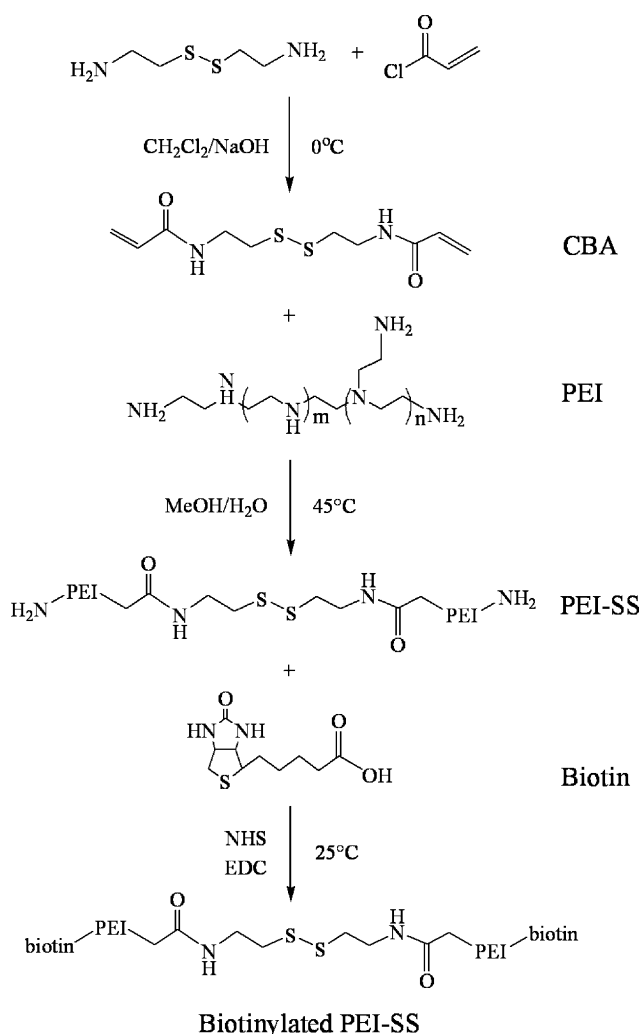
Key Laboratory of Biomedical Polymers of Ministry of Education & Department of Chemistry, Wuhan University, Wuhan, 430072, P. R. China. E-mail: xz-zhang@whu.edu.cn; Fax: +86 27 6875 4509; Tel: +86 27 6875 4061

observation, particle size and  $\zeta$ -potential measurements, and PEI-SS was used as the control. The toxicity and transfection efficiency of ABP-SS in different cells were studied, moreover, the pDNA tracking assay was investigated by confocal laser scanning microscopy.

## Results and discussions

### Synthesis and characterization of biotinylated PEI-SS

In this study, PEI-SS was synthesized from the Michael addition between CBA and branched 800 Da PEI according to our previous work,<sup>4</sup> and then biotin was linked to PEI-SS using EDC. The synthesis route for BP-SS is illustrated in Scheme 1. The product was purified twice by exhaustive dialysis in a dialysis tube (MWCO: 3500) to remove the residues of solvent, the unreacted 800 Da PEI as well as free biotin.



The structures of products were confirmed by  $^1\text{H}$  NMR spectroscopy, and the spectra of biotin, PEI-SS and BP-SS are shown in Fig. 1. The characteristic peaks of biotin in  $\text{D}_2\text{O}$  solvent appeared at  $\delta$  1.3–1.5 ppm,  $\delta$  2.6–3.2 ppm and  $\delta$  4.4 ppm (Fig. 1(A) *H1*–*H6*). For PEI-SS, the peaks between  $\delta$  2.5 and 3.0 ppm in  $^1\text{H}$  NMR

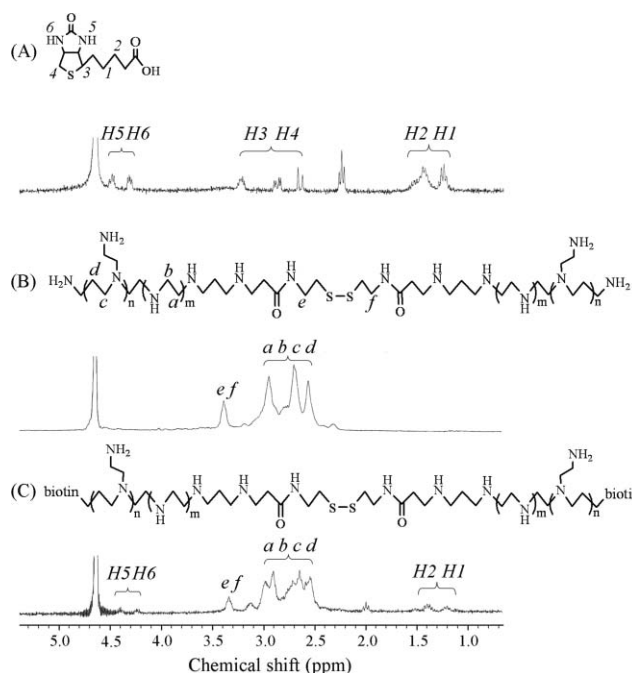


**Fig. 1**  $^1\text{H}$  NMR spectrum of biotin (A), PEI-SS (B) and biotinylated PEI-SS (C) in  $\text{D}_2\text{O}$ .

spectra belonged to the special shift of branched PEI (Fig. 1(B) *a*–*d*), and the peak near  $\delta$  3.3 belonged to  $\text{CH}_2\text{-SS-CH}_2$  protons of PEI-SS (Fig. 1(B) *e*, *f*). As shown in Fig. 1(C), although the *H3* and *H4* peaks of biotin were overlapped by the characteristic peaks of PEI (*a*–*d*), the *H1*, *H2*, *H5* and *H6* peaks of biotin appeared in  $^1\text{H}$  NMR spectra of BP-SS, indicating that biotin was successfully linked to PEI-SS. Biotin to PEI-SS ratio was calculated based on integrations with respect to the  $\text{CH}_2$  protons of biotin (*H1*, *H2*), the  $\text{CH}_2\text{-SS-CH}_2$  protons of PEI-SS (*e*, *f*) and the  $\text{CH}_2$  protons of PEI (*a*–*d*). According to  $^1\text{H}$  NMR spectra, it can be calculated that one 800 Da PEI molecule was coupled with 1.27 biotin molecules. The number average molecular weights ( $M_n$ ) of PEI-SS was 9.65 kDa measured by GPC (PDI = 1.96).

### Gel retardation assay

The binding capability of polycation to pDNA is a prerequisite for the gene vector. The ability of ABP-SS and PEI-SS to condense pDNA was assessed through the elimination of electrophoretic mobility using agarose gel electrophoresis at various N/P ratios ranging from 0 to 30. DNA bands of ABP-SS and PEI-SS are strong and clear in sample wells at N/P ratio 6 to 30 in Fig. 2A and B, indicating that pDNA can be fully condensed at these N/P ratios and could be used in the following transfection study. Moreover, because the gel retardation assay was operated during a period of time, the plasmid DNA degraded slightly, this made the second band of free plasmid stronger in Fig. 2A and B.

It is known that glutathione is a tripeptide found within cells at millimolar concentrations as a water-soluble reducing agent that can degrade disulfide-containing polymers to the corresponding thiols.<sup>11</sup> In this experiment, another SH-reducing agent (DTT) was used as glutathione to simulate and investigate the degradation of polymers. Fig. 2 shows the effect of DTT on the binding capability of polymer/DNA complexes. Generally, the hazy luminescent

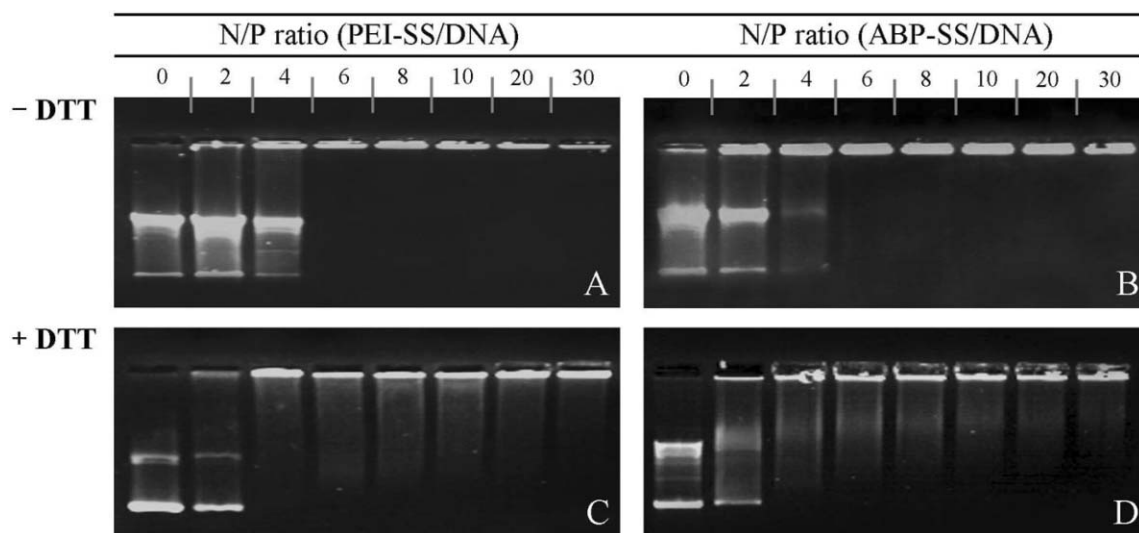


**Fig. 2** Agarose gel electrophoresis retardation assay of polymer/DNA complexes which were prepared at different N/P ratio: 0, 2, 4, 6, 8, 10, 20, 30; and were separated on a 0.7% agarose gel. (A) PEI-SS/DNA complexes, (B) ABP-SS/DNA complexes without DTT and (C) PEI-SS/DNA complexes, (D) ABP-SS/DNA complexes with 50 mM DTT. The leftmost lane (N/P = 0) shows the mobility of plasmid only used as a control.

bands below the immobilized DNA were considered as the migration of released DNA. The migration of DNA was observed obviously at N/P ratios ranging from 6 to 30 when the complexes incubated with 50 mM DTT (Fig. 2C and D). It was inferred that, in the presence of DTT, ABP-SS and PEI-SS were degraded within 30 min which led to the release of free DNA. In consequence, upon the reducing condition of cytoplasm, the condensed DNA would release from the complexes easily, allowing the increasing uptake of DNA and enhancing transgene expression inside the nucleus.

### Buffer capability

The buffer capability of a gene vector is very important for complexes escaping from the endosomes and promoting transfection efficacy. It is reported that PEI and its derivatives contain varying levels of 1°, 2° and 3° amines that can become protonated under a pH range, giving rise to the so-called “proton sponge” effect that may contribute to the high efficiency of PEI as a gene delivery vehicle.<sup>2</sup> In this study, the buffer capabilities of PEI (25 kDa and 800 Da), PEI-SS and ABP-SS were evaluated by acid-base titration in 150 mM NaCl solution. As shown in Fig. 3, buffer capability curves of PEI (25 kDa and 800 Da) and ABP-SS were quite approximate, however, that of PEI-SS was relatively lower. Because avidin is a basic glycoprotein with an unusually high isoelectric point ( $I_p$ ) at pH = 10.5,<sup>6</sup> so that it will be protonated and present positive charge and when pH <  $I_p$  (such as pH = 7.4). Accordingly, avidin could enhance the pH buffer capability. Hence, ABP-SS presented very good protonation capability as well as 25 kDa PEI, which made the complexes escape from endosomes easier and faster during the transfection process.

### Particle size and $\zeta$ -potential measurement

The ability of a polymer to condense DNA can be evaluated by particle size and  $\zeta$  potential measurements. In this study,

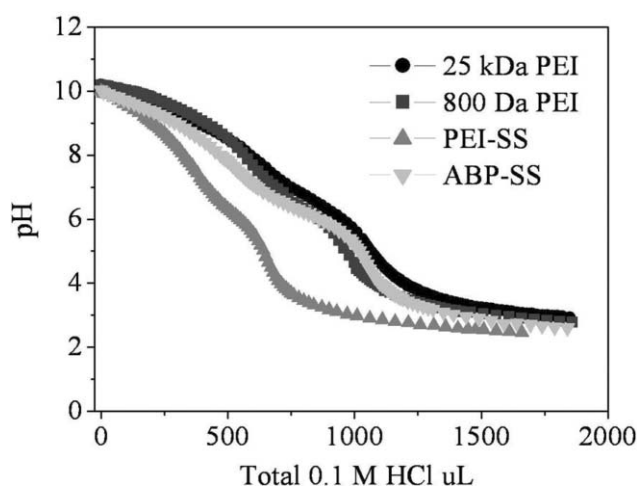


**Fig. 3** Acid-base titration profiles of 25 kDa PEI, 800 Da PEI, PEI-SS and ABP-SS in 150 mM NaCl solution.

the particle sizes of ABP-SS/pDNA complexes at various N/P ratios ranging from 5 to 120 were measured by adding ABP-SS solution to 1  $\mu$ g pDNA at physiological ionic strength conditions (in 150 mM NaCl solution). PEI-SS was used as the control. As presented in Fig. 4a, a mild rise of particle size of both complexes could be seen when the N/P ratio increased from 5 to 40, so it could be considered that polycation molecules were attracted by DNA and led to aggregates among those small complexes when polymer concentration was slightly increased. However, particle sizes of both complexes dropped sharply accompanied by the continuously increasing N/P ratios (such as N/P ratio = 80 and 120), which was accordant with the results of the former report by Sun.<sup>4</sup> Compared with the PEI-SS, although particle sizes of ABP-SS/pDNA complexes were slightly larger at each N/P ratio attributed to the high molecular weight of avidin (the data show no significant difference), avidin could give pDNA better protection from enzyme inhibition during gene delivery. The mean particle

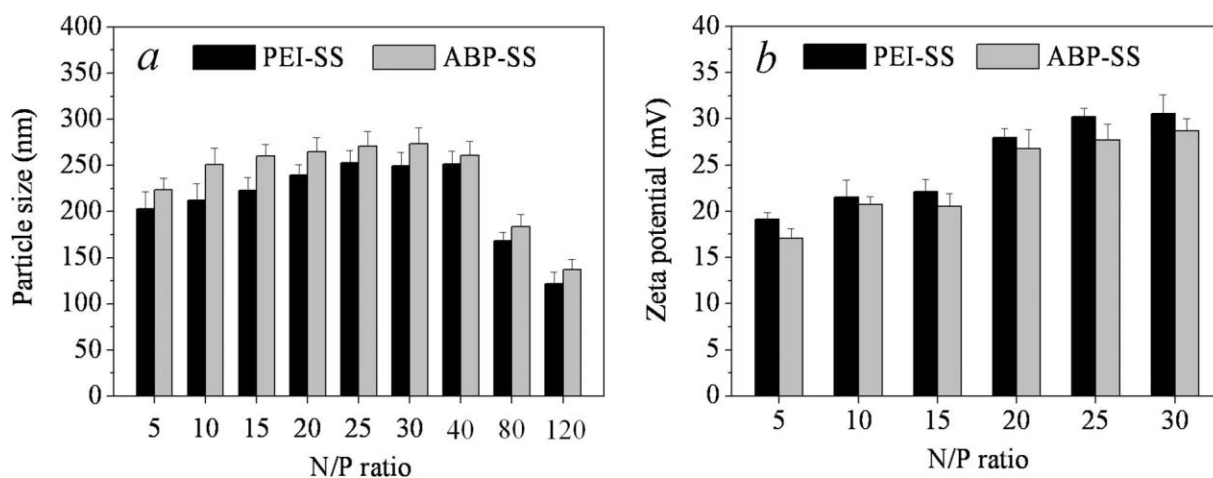


**Fig. 4** Particle size (a) and  $\zeta$ -potential (b) of ABP-SS/DNA complexes at various N/P ratios. PEI-SS was used as a control. Data were shown as mean  $\pm$  SD (n = 3).

size of ABP-SS/pDNA complexes was  $226 \pm 40$  nm, while that of PEI-SS/pDNA complexes was  $205 \pm 40$  nm.

The positively charged complex is essential for binding the negatively charged cellular membrane, which facilitates the entering of a complex into the nucleolus by cellular uptake.<sup>2</sup> The  $\zeta$ -potential values of polymer/pDNA complexes were also measured at N/P ratios ranging from 5 to 30. Fig. 4b reveals that the  $\zeta$ -potential values of ABP-SS/pDNA and PEI-SS/pDNA complexes had a similar trend and experienced constant growth with the increasing N/P ratios. The average  $\zeta$ -potentials of both complexes were about  $25 \pm 5$  mV. Compared with the PEI-SS, ABP-SS/pDNA complexes revealed a slight drop at each N/P ratio, suggesting that avidin with a low positive charge may reduce the surface charges of PEI-SS (the data show no significant difference). It is generally believed that a high surface charge enhances the interaction of the complex with the negatively charged cell membrane,<sup>2</sup> and the positive  $\zeta$ -potentials could stabilize the complexes against aggregation and guarantee a small complex size. However, a higher positive surface charge directly increases the cytotoxicity of the polycation, which may reduce the transfection efficacy and limit the clinical applications. Accordingly, ABP-SS/pDNA complexes with a lower positively charged surface displayed lower cytotoxicity in comparison with PEI-SS/pDNA complexes.

### SEM morphology observation

Based on the results of particle size for all the complexes (Fig. 4a), ABP-SS and BP-SS complexed with pDNA at two different N/P ratios (10 and 30) were evaluated respectively *via* SEM morphology. As shown in Fig. 5, the typical images showed that the complexes had compact structures with spherical or quadrate shapes. Moreover, the SEM images demonstrated that the size of the complexes were about 200–400 nm in accordance with the results measured by Nano-ZS ZEN3600. These results showed that ABP-SS would condense pDNA compactly as well as PEI-SS. Additionally, it can be observed that the sizes of complexes at N/P of 30 (Fig. 5B and D) were larger than that of complexes at N/P of 10 (Fig. 5A and C), indicating that higher polymer contents enlarge the particle size of the complexes when the N/P ratio is

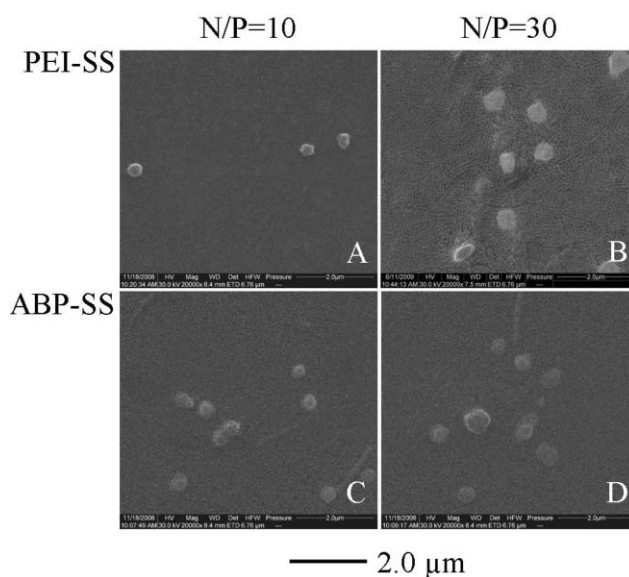


**Fig. 5** SEM of ABP-SS and PEI-SS complexed with pDNA. (A) PEI-SS/pDNA complexes at N/P = 10; (B) PEI-SS/pDNA complexes at N/P = 30; (C) ABP-SS/pDNA complexes at N/P = 10; (D) ABP-SS/pDNA complexes at N/P = 30. The micrographs are obtained at magnification of 20000 $\times$ .

less than 30. Because aggregation would happen during the drying process of SEM sample, complexes observed by SEM are larger than those from particle size measurement.

### In vitro cytotoxicity

The cytotoxicity of the gene vector is definitely essential to the clinical application, which strongly depends on the biocompatibility of the material. In order to evaluate the potential toxicity of ABP-SS and PEI-SS, the viabilities of three different cell lines, HepG2, 293T and H446 cells, were tested by MTT assay. 25 kDa PEI was used as the control. As shown in Fig. 6, both ABP-SS and PEI-SS maintained relatively high cell viabilities (more than 60%) in all cell lines, in contrast, the cytotoxicity curves of 25 kDa PEI presented sharp drops during the whole concentration range. In addition,



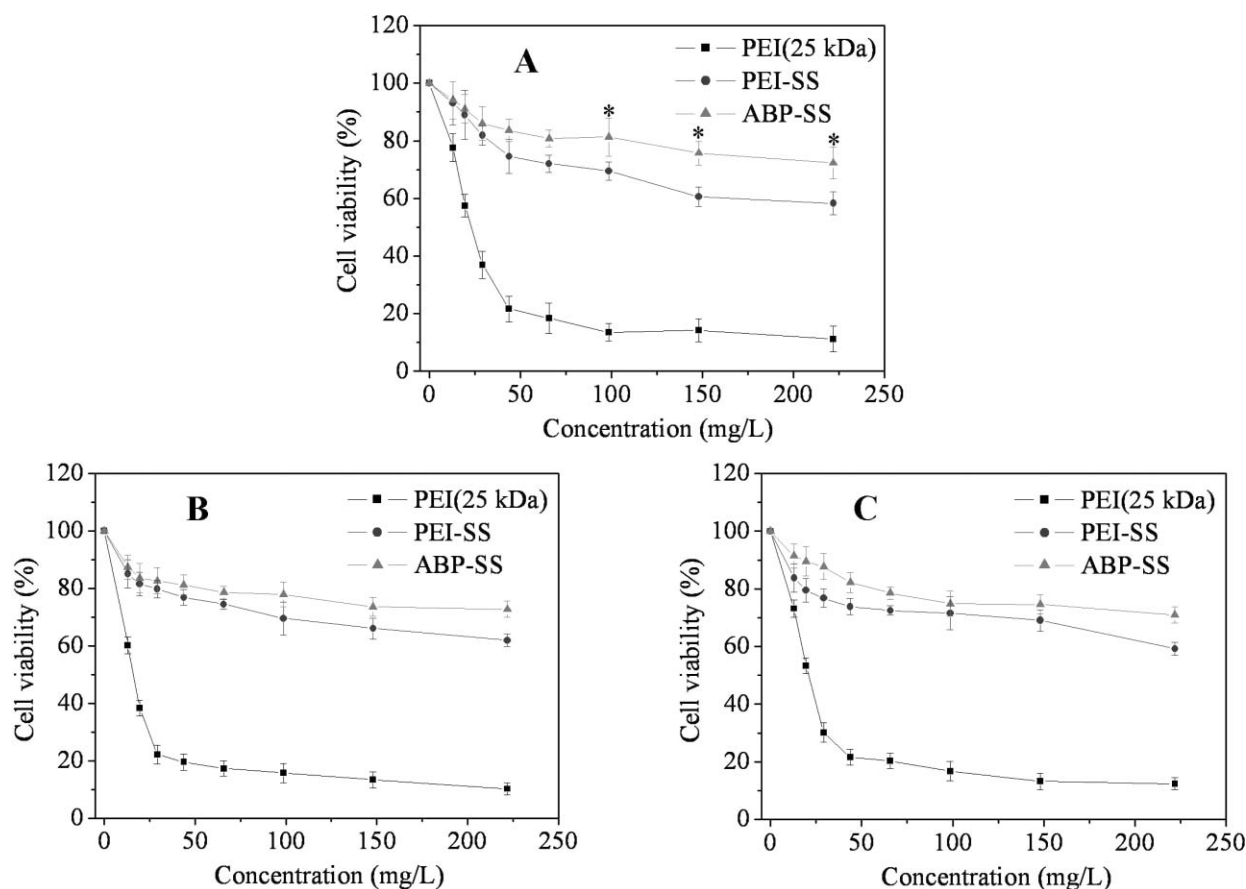


**Fig. 6** Cytotoxicity induced by ABP-SS in comparison to with PEI-SS and 25 kDa PEI in (A) HepG2, (B) 293T and (C) H446 cells. The X-axis indicates the polymer concentrations, while the Y-axis shows the cell percentile viability. The relative cell viability was compared with the untreated cells. Data are shown as mean  $\pm$  SD ( $n = 3$ ). (\*:  $p < 0.05$  as compared with the data of PEI-SS).

ABP-SS demonstrated obviously higher cell viabilities than PEI-SS at higher polymer concentrations, especially in HepG2 cells (Fig. 6(A),  $*p < 0.05$ ). This is attributed to the introduction of biotins and avidins, which might reduce the surface charge intensity of polycation and benefit to the bioactivity of cells. It is suggested that there might exist somewhat specific interactions between avidin and HepG2 cells, which made the polycation vector more ecological, biocompatible and less toxic.

#### *In vitro* transfection

The transfection efficiencies of ABP-SS/pDNA and PEI-SS/pDNA complexes were assessed in HepG2 cells, 293T cells and H446 cells at N/P ratio ranged from 5 to 30 (Fig. 7 and 8). As shown in Fig. 7(A), ABP-SS/pDNA complexes presented much higher transfection levels than PEI-SS/pDNA complexes in HepG2 cells over the whole N/P ratio range. For example, the transgene expression of ABP-SS/pDNA complexes at N/P ratio of 5 ( $3.61 \times 10^8$  RLU/mg protein, Fig. 7A,  $*p < 0.05$ ) was statistically significantly higher than that of PEI-SS at the same N/P ratio ( $5.67 \times 10^6$  RLU/mg protein). This suggests that the presence of the avidin component facilitated the transfection of the ABP-SS/pDNA complex in the HepG2 cells. Moreover, the ABP-SS/pDNA complex at N/P ratio of 10 presented much higher transfection efficacy than the 25 kDa PEI control, indicating that

ABP-SS was an efficient gene vector for HepG2 cell transfection. In 293T cells (Fig. 7B), the transfection ability of ABP-SS was quite similar to that of PEI-SS. The transgene expression of ABP-SS/pDNA complexes at N/P ratio of 15 ( $3.29 \times 10^8$  RLU/mg protein) was comparable to that of PEI-SS/pDNA complexes at the same N/P ratio ( $3.67 \times 10^8$  RLU/mg protein). With respect to H446 cells (Fig. 7C), the transfection efficiency of ABP-SS/pDNA complexes was slightly lower than that of PEI-SS/pDNA complexes at each N/P ratio (no significant difference). For 293T and H446 cells, ABP-SS/pDNA complex at N/P ratio of 10 presented comparable transfection efficacy with the 25 kDa PEI control. According to these results, it can be inferred that ABP-SS was a desirable gene vector and also displayed specific transfection capability in HepG2 cells rather than 293T or H446 cells.

The green fluorescent protein expressions of ABP-SS/pDNA and PEI-SS/pDNA complexes at the optimal N/P ratio of 10 in HepG2 cells, H446 cells and 293T cells are shown in Fig. 8. For HepG2 cells, the strong fluorescent density could be seen when cells were transfected with ABP-SS/pDNA complexes (Fig. 8b<sub>1</sub>), whereas the weak fluorescent density was displayed when cells were transfected with PEI-SS/pDNA complexes (Fig. 8a<sub>1</sub>). On the contrary, as for H446 cells and 293T cells, the fluorescent densities had not shown obvious difference between ABP-SS/pDNA complexes and PEI-SS/pDNA complexes (Fig. 8c<sub>1</sub>-f<sub>1</sub>). These images further

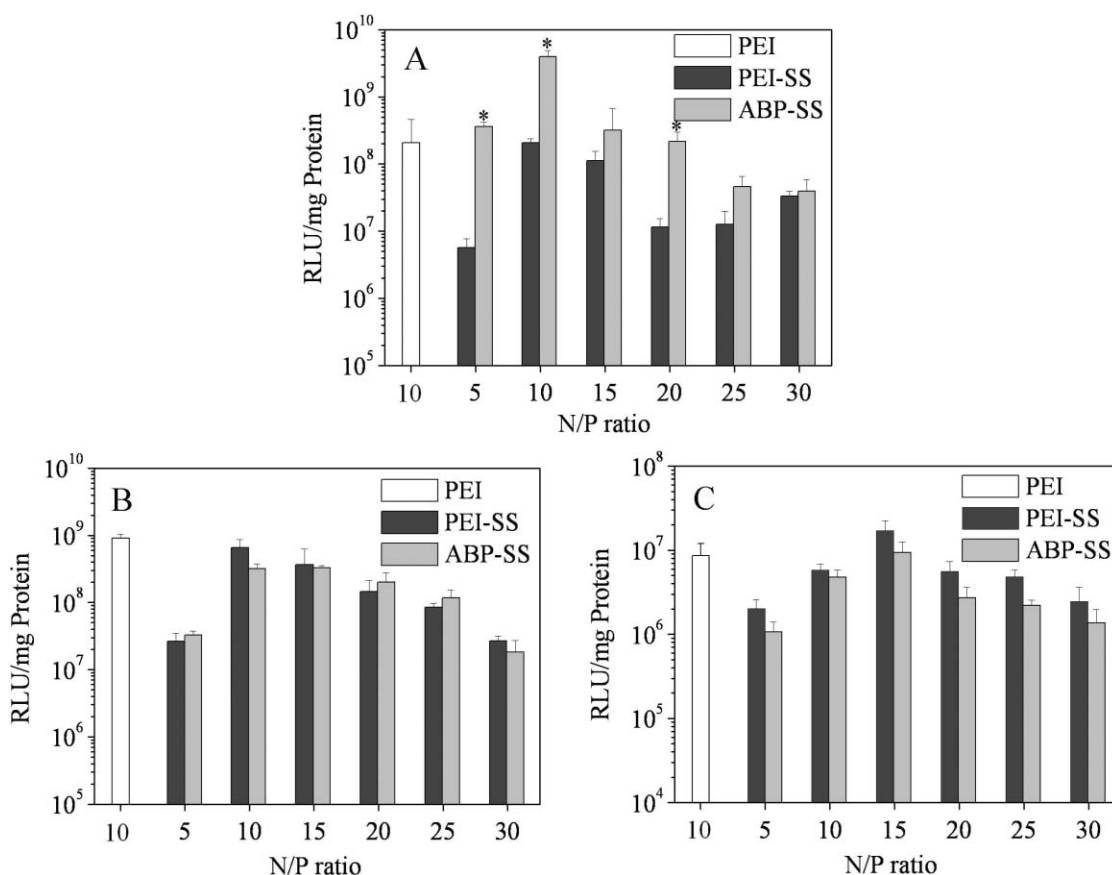


**Fig. 7** Transfection efficiency of ABP-SS/pDNA and PEI-SS/pDNA complexes at N/P ratios ranging from 5 to 30 in (A) HepG2, (B) 293T and (C) H446 cells. Data are shown as mean  $\pm$  SD ( $n = 3$ ). (\*:  $p < 0.05$  as compared with the data of PEI-SS).

proved that the transfection efficiency was greatly enhanced by ABP-SS compared with PEI-SS only in HepG2 cells.

The probable mechanism for transfection enhancement in HepG2 cells could be explained as follows: pDNA was condensed with ABP-SS which had better biocompatibility, and it can be speculated that some specific interactions existed between avidin and HepG2 cells which could be considered as a special targeting. After binding to the cell surface, ABP-SS/pDNA complexes were internalized, escaped from the endosome and translocated to the nucleus where genes were expressed. Enhanced cell interaction led to more particle uptake and greater gene expression.

#### Cellular uptake

To illuminate the cellular uptake of complexes in HepG2 cells, 293T cells and H446 cells, molecular probes (YOYO-1 and Hoechst 33258) were used to tag DNA and nucleus. Turquoise fluorescence (overlapped by blue and green fluorescence) can be seen in Fig. 9, which indicated that YOYO-1 labeled complexes were accumulated in the nucleus of cells (white arrows). For HepG2 cells, compared with Fig. 9a<sub>2</sub>, much more turquoise fluorescence could be observed evidently in Fig. 9a<sub>1</sub>, which indicated that cellular uptake in HepG2 cells was markedly enhanced by ABP-SS and plasmid DNA were successfully transported into the nucleus of HepG2 cells. The endocytosis of ABP-SS/pDNA complexes was significantly higher compared with that of PEI-SS/pDNA

complexes. However, as shown in Fig. 9b<sub>1</sub> and b<sub>2</sub>, less turquoise fluorescence of ABP-SS/pDNA complexes could be seen in 293T cells as well as PEI-SS/pDNA complexes. Moreover, only a few turquoise fluorescent dots were found in H446 cells transfected by both complexes (Fig. 9c<sub>1</sub> and c<sub>2</sub>), which was probably attributed to the fluid phase pinocytosis. These results demonstrated that ABP-SS contributed to more cellular uptake of complexes in HepG2 cells, which was also consistent with the results of transfection efficiency.

#### Conclusions

In conclusion, we synthesized a targeting gene vector, biotinylated disulfide containing polyethyleneimine/avidin bioconjugate (ABP-SS), which presented less toxic and higher gene expression, especially in HepG2 cells. This was accomplished by grafting biotin to disulfide-containing polyethylenimine (PEI-SS) and bioconjugating with avidin by the avidin-biotin strong affinity. The resulted gene vector ABP-SS and its pDNA complexes were evaluated in terms of gel retardation assay, SEM, particle size,  $\zeta$ -potential, *in vitro* cell viability and transfection efficiency. Results indicated that ABP-SS, compared with PEI-SS, demonstrated significant lower cytotoxicity and much higher transfection efficacy in HepG2 cells due to the biocompatibility of avidin and the specific interactions between avidin and HepG2 cells. ABP-SS provided a promising potential in targeting gene delivery to liver cells and could also be useful for other forms of hepatic disease.

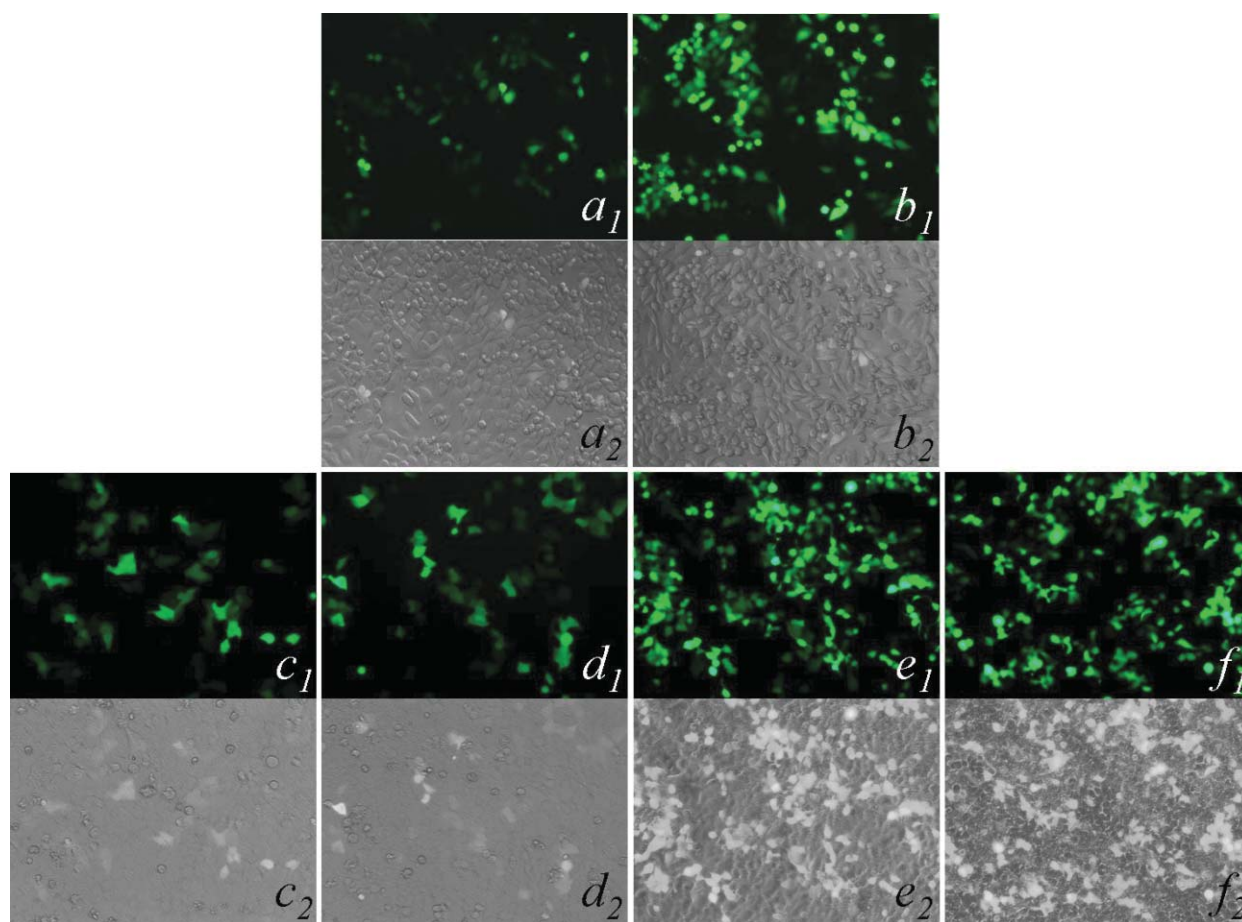


**Fig. 8** The fluorescence images of HepG2, H446 and 293T cells transfected by the complexes of pEGFP and ABP-SS or PEI-SS at N/P = 10. PEI-SS (a, c, e), ABP-SS (b, d, f), HepG2 cells (a, b), H446 cells (c, d), 293T cells (e, f), green fluorescence image ( $a_1$ ,  $b_1$ ,  $c_1$ ,  $d_1$ ,  $e_1$ ,  $f_1$ ), bright field image ( $a_2$ ,  $b_2$ ,  $c_2$ ,  $d_2$ ,  $e_2$ ,  $f_2$ ). The micrographs are obtained at magnification of 100 $\times$ .

## Experimental

### Materials

Branched polyethylenimine (PEI) with molecular weight of 25 kDa and 800 Da, cystamine dihydrochloride (98%), d-biotin, N-hydroxysuccinimide (NHS) and N-ethyl-N'-(3-dimethylaminopropyl) carbodiimide (EDC) were purchased from Sigma-Aldrich (Steinheim, Germany). Acryloyl chloride of analytical grade and 1,4-dithiothreitol (DTT) were purchased from Shanghai Chemical Reagent Co. (Shanghai, China) and used as received. Avidin with molecular weight of 66 kDa was purchased from Pierce (Rockford, IL, USA). Dimethyl sulfoxide (DMSO) was obtained from Shanghai Chemical Reagent Co. (Shanghai, China) which was dried by refluxing with anhydrous  $\text{MgSO}_4$  overnight and was then distilled under reduced pressure. QIAfilter<sup>TM</sup> plasmid purification Giga Kit (5) was purchased from Qiagen (Hilden, Germany). GelRed<sup>TM</sup> was purchased from Biotium (CA, USA). Molecular probes (YOYO-1 and Hoechst 33258) were purchased from Invitrogen (CA, USA). Dulbecco's Modified Eagle's Medium (DMEM), fetal bovine serum (FBS), penicillin-streptomycin, trypsin, 3-(4,5-dimethylthiazol-2-yl)-2,5-diphenyltetrazolium bromide (MTT), and Dulbecco's phosphate buffered saline (PBS) were purchased from Invitrogen (CA, USA). The Micro BCA protein assay kit was purchased from

Pierce (Rockford, IL, USA). All other reagents were analytical grade and used as received. 150 mM NaCl solution was used to mimic the physiological saline environments.<sup>5</sup>

### Synthesis of cystamine bisacrylamide (CBA)

The synthesis was according to the literature.<sup>12</sup> In brief, cystamine dihydrochloride (0.025 mol, 5.3 g) was dissolved in water (25 mL) and added to a three-necked flask. After the solution was cooled to 0–5 °C, an acryloyl chloride dichloromethane solution (0.1 mol, 5 mL) and an aqueous NaOH solution (0.2 mol, 10 mL) were added simultaneously at 0–5 °C. After the solution addition was completed, the reaction mixture was stirred continuously at room temperature for 16 h, and a suspended solution was obtained. Then the white raw product was obtained by filtration and washed 3 times with water. The raw product was further purified by crystallization using acetate. Finally, the white solid, prepared CBA was obtained by removing the solvent under vacuum.

### Synthesis of disulfide-containing polyethylenimine (PEI-SS)

The reducible PEI-SS was synthesized by Michael addition between CBA and low molecular weight branched 800 Da PEI according to the literature.<sup>4</sup> Briefly, 0.86 g of PEI was dissolved in 10 mL 10% aqueous methanol and then added to a three-necked



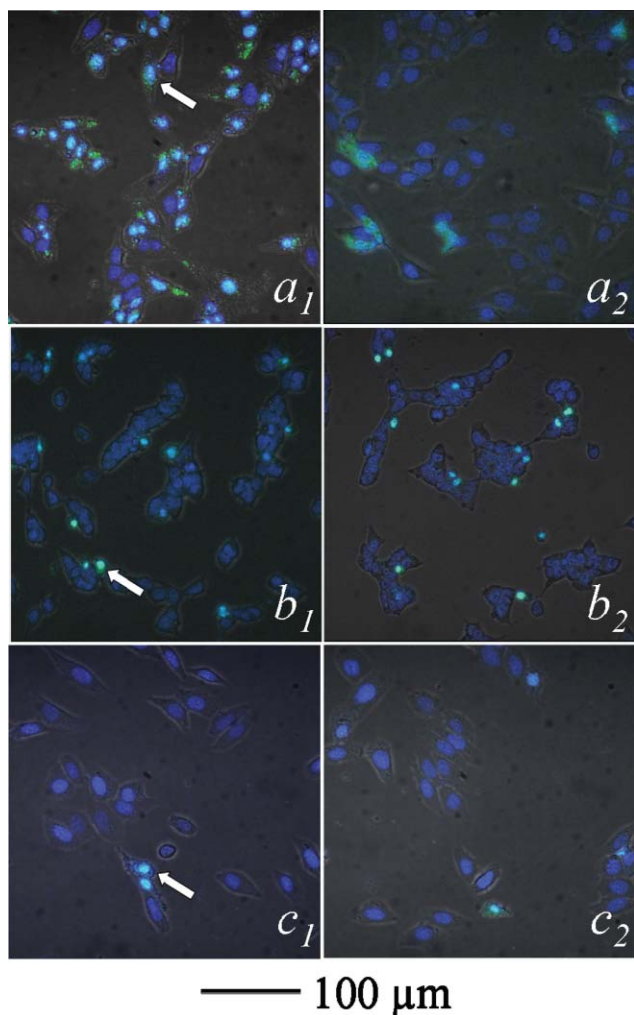


**Fig. 9** Confocal overlapped images of HepG2 (a), 293T (b) and H446 (c) cells after incubation with the complexes of pGL-3 and ABP-SS ( $a_1$ ,  $b_1$ ,  $c_1$ ) or PEI-SS ( $a_2$ ,  $b_2$ ,  $c_2$ ). pGL-3 plasmids are stained green by YOYO-1. Nucleus of cells is stained blue by Hoechst 33258. The micrographs are obtained at magnification of 400 $\times$ .

flask equipped with a condenser at 45 °C under a nitrogen atmosphere. To obtain the PEI-SS with a molar ratio of 1:2 between the reactive group in CBA and the primary amine in PEI respectively, 0.325 g CBA was dissolved in 6 mL methanol respectively and dropwise added to the PEI solution. The reaction mixture was stirred in the dark under nitrogen atmosphere for at least 24 h at 45 °C. Subsequently, 10% excess PEI (0.086 g) in 2 mL methanol was added to consume any unreacted acrylamide groups for another 6 h with stirring. After that the transparent solution was diluted with water to 20 mL and acidified with 10 M HCl to pH 4, and then dialyzed against distilled water (MWCO: 3500) for 2 days to remove the unreacted 800 Da PEI. Lastly, the solution was lyophilized for 2 days to obtain the product.

#### Synthesis of biotinylated PEI-SS

The biotinylated PEI-SS (BP-SS) was prepared according to the literature.<sup>6</sup> Biotin (30 mg) was activated with NHS (14 mg) and EDC (23 mg) in dimethyl sulfoxide (3 mL). The activated biotin solution was added to PEI-SS (200 mg) in deionized water (12 mL).

The reaction mixture was stirred at 4 °C for 24 h, purified by dialyzing against water for 2 days (MWCO: 3500), lyophilized and defined as BP-SS.

#### Polymer characterizations

<sup>1</sup>H Nuclear Magnetic Resonance Spectroscopy (NMR) of prepared CBA, PEI-SS and BP-SS were recorded on a Varian Unity 300 MHz spectrometer with CDCl<sub>3</sub> and D<sub>2</sub>O as the solvent respectively. The molecular weights and polydispersity (M<sub>w</sub>/M<sub>n</sub>) of the PEI-SS determined by Gel Permeation Chromatography (GPC) relative to PEG standards using a Waters-2690D HPLC equipped with Ultrahydrogel 120 and 250 columns. HAc-NaAc buffer solution (0.03 M, pH 2.8) was used as eluent at a flow rate of 1.0 mL/min.

#### Biotinylated PEI-SS conjugates with avidin

The appropriate amount of avidin was dissolved in 150 mM NaCl, and then 20-fold weight excess of BP-SS was added. The mixture was vortexed and reacted at room temperature for 30 min to obtain the ABP-SS solution.

#### Cell culture

Human hepatoblastoma cells (HepG2), human embryonic kidney transformed 293 cells (293T) and human small cell lung cancer cells (H446) were incubated in DMEM supplemented with 10% FBS and 1% antibiotics (penicillin-streptomycin, 10,000 U/mL) at 37 °C in a fully humidified atmosphere of 5% CO<sub>2</sub>.

#### Amplification and purification of plasmid DNA

Luciferase (pGL-3) and expressing green fluorescent protein (pEGFP-N1) plasmids were used in this study. The former one as the luciferase reporter gene was transformed in *E. coli* JM109 and the latter one as the green fluorescent protein gene was transformed in *E. coli* DH5 $\alpha$ . Both plasmids were amplified in terrific broth media at 37 °C overnight at 250 rpm. The plasmids were purified by an EndoFree QiAfilter™ Plasmid Giga Kit (5). Then the purified plasmid were dissolved in TE buffer solution and stored at -20 °C. The integrity of plasmid was confirmed by agarose gel electrophoresis. The purity and concentration of plasmid were determined by ultraviolet (UV) absorbance at 260 and 280 nm.

#### Acid-base titration

The buffer capability of 25 kDa PEI, 800 Da PEI, BP-SS and ABP-SS were determined by acid-base titration assay over the pH from 10 to 2 as described by Benms *et al.*<sup>13</sup> Briefly, 0.2 mg/mL of each sample solution was prepared in 30 mL 150 mM NaCl solution. The sample solution was first titrated by 0.1 M NaOH to a pH of 10, then different volumes of 0.1 M HCl were added to the solution, and the different pH values were measured using a microprocessor pH meter.

#### Agarose gel retardation assay

The ABP-SS/pDNA and PEI-SS/pDNA complexes at different N/P ratios range from 0 to 30 (the primary amino groups of PEI



in the PEI-SS to phosphate groups of pDNA) were prepared by adding appropriate volume of BP-SS solution (in 150 mM NaCl solution) to 1  $\mu$ L of pEGFP-N1 pDNA (100 ng/ $\mu$ L in 40 mM Tris-HCl buffer solution) with or without 50 mM DTT. The complexes were diluted by 150 mM NaCl solution to a total volume of 6  $\mu$ L, and then the complexes were incubated at 37 °C for 30 min. After that the complexes were electrophoresed on the 0.7% (W/V) agarose gel containing GelRed™ and with Tris-acetate (TAE) running buffer at 80 V for 80 min. pDNA was visualized with a UV lamp using a Vilber Lourmat imaging system (France).

### Particle size and $\zeta$ -potential measurement

The particle size and  $\zeta$ -potential were measured by Nano-ZS ZEN3600 (MALVERN Instr.) at 25 °C. The complexes at various N/P ratios range from 5 to 120 were prepared by adding the appropriate volume of ABP-SS solution or PEI-SS solution (in 150 mM NaCl solution) to 1  $\mu$ g of pGL-3 pDNA (in 40 mM Tris-HCl buffer solution). After that the complexes were diluted by 150 mM NaCl solution for particle measurement or diluted by distilled water for  $\zeta$ -potential measurement to 1 mL. Then the complexes were incubated at 37 °C for 30 min.

### Scanning electron microscopy (SEM)

The morphologies of ABP-SS/pDNA complexes and PEI-SS/pDNA complexes at N/P = 10 and 30 were observed respectively by SEM (FEI-QUANTA 200). The complexes were prepared by adding 1  $\mu$ g of pDNA (in water) to the appropriate volume of ABP-SS solution (in water) and PEI-SS solution (in water), respectively. The complexes were diluted to a total volume of 100  $\mu$ L by water and then incubated at 37 °C for 30 min. The SEM samples were prepared by dropping the polymer/pDNA complexes solution onto the glass slip and then kept in aseptic manipulation cabinet at 30 °C for 2 h for drying. Before SEM observation, the samples were coated with gold for 7 min. The micrographs of complexes were obtained at magnification of 40,000 $\times$ .

### Cytotoxicity assay

The cytotoxicity of ABP-SS and PEI-SS were examined by MTT assay, 25 kDa PEI were used as the control. The HepG2, 293T and H446 cells were seeded respectively in the 96-well plates at a density of 6000 cells/well and cultured 24 h in 200  $\mu$ L DMEM containing 10% FBS. After that, the polymers were added for 2 days and the medium was replaced with 200  $\mu$ L of fresh medium. Then 20  $\mu$ L MTT (5 mg/mL) solutions were added to each well and further incubated for 4 h. Thereafter, the medium was removed and 150  $\mu$ L DMSO was added. The absorbance of color was measured at 570 nm by a microplate reader (BIO-RAD, Model 550, USA). The relative cell viability was calculated according to the following equation: Cell viability (%) =  $[\text{OD}_{570}(\text{samples})/\text{OD}_{570}(\text{control})] \times 100$ , where  $\text{OD}_{570}(\text{control})$  was obtained in the absence of polymers and  $\text{OD}_{570}(\text{samples})$  was obtained in the presence of polymers.

### In vitro transfection

Transfection experiments of ABP-SS and PEI-SS were performed with HepG2, 293T and H446 cells, and 25 kDa PEI was used

as the control. Both pGL-3 and pEGFP-N1 plasmid DNA were utilized to evaluate the transfection efficiency. Cells were seeded at a density of  $6 \times 10^4$  cells/well in the 24-well plate with 1 mL of DMEM containing 10% FBS and incubated at 37 °C for 24 h. The complexes were prepared at N/P ratios ranging from 5 to 30 by adding the appropriate volume of polymer solution to 1  $\mu$ g plasmid DNA per well, and then incubated at 37 °C for 30 min. Then the polymer/pDNA complexes were added into the plate with serum-free DMEM at 37 °C for 4 h. After that, the serum-free DMEM was replaced with fresh DMEM containing 10% FBS and the cells were further incubated for 2 days. For luciferase assay, the medium was removed and cells were washed by PBS, then the cells were lysed using 200  $\mu$ L reporter lysis buffer (Pierce). The relative light units (RLUs) were measured with a chemiluminometer (Lumat LB9507, EG & G Berthold, Germany). The total protein was measured according to a BCA protein assay kit (Pierce) and luciferase activity was expressed as RLU/mg protein. The cells expressing green fluorescent proteins were directly observed by an inverted microscope (IX 70, Olympus, Japan). The micrographs were obtained at the magnification of 100 $\times$  and recorded using CoolSNAP-Pro (4.5.1.1) version software.

### Cellular uptake study

Live cell confocal microscopy was used to image ABP-SS/pDNA and PEI-SS/pDNA complex uptake into HepG2, 293T and H446 cells. 10  $\mu$ M YOYO-1 water stock solution (green molecular probe) was used to tag pGL-3 and 10 mg/mL Hoechst 33258 water stock solution (blue molecular probe) was used to stain nucleus. Cells were seeded into LabTek chamber slide dishes at a density of  $5.0 \times 10^4$  cells/well with 1 mL of DMEM containing 10% FBS and incubated at 37 °C for 24 h. 1  $\mu$ g pGL-3 plasmid was mixed with 2.5  $\mu$ L YOYO-1 solution and incubated for 15 min at 37 °C. Then the complexes were prepared at an N/P ratio of 10 by adding appropriate volume of ABP-SS solution to the YOYO-1 labeled pGL-3 and incubated for 30 min at 37 °C. After the complexes were added into the wells of a cell plate and incubated in serum-free DMEM for 4 h at 37 °C, the serum-free DMEM was removed, the cells in each well were washed twice with PBS, and then 200  $\mu$ L DMEM (with FBS) with 20  $\mu$ L Hoechst 33258 solution was added and incubated for 20 min at 37 °C. Finally, the solution was removed, cells in each well were washed with PBS twice, and 1 mL fresh DMEM (with FBS) was added. The fluorescent images of cells were observed under excitation at 488 nm using confocal laser scanning microscopy (Nikon C1-si TE2000, Japan). The micrographs of cells were obtained at the magnification of 400 $\times$  and recorded using EZ-C1 FreeViewer 3.70 version software. The control experiment was also carried out under the same condition by the use of PEI-SS. All confocal images were slice images to distinguish ABP-SS or PEI-SS internalized from that adherent to the outside cellular membrane. The whole preparation process should avoid exposure to strong light in order to protect the fluorescent dyes.

### Statistical analysis

The results are representative of replicate experiments performed with a sample size equal to three or four in each experiment, as indicated on the figure legend. The results are represented by

the mean and standard deviation. All statistical analyses were performed using Student's t-test. Probability values less than 0.05 ( $P < 0.05$ ) were considered to be indicative of statistical significance.

## Acknowledgements

Acknowledgement is made to National Natural Science Foundation of China (50633020), National Key Basic Research Program of China (2005CB623903) and Ministry of Education of China (Cultivation Fund of Key Scientific and Technical Innovation Project 707043).

## References

- (a) S. Li and L. Huang, *Gene Ther.*, 2000, **7**, 31; (b) T. Niidome and L. Huang, *Gene Ther.*, 2002, **9**, 1647; (c) Y. Kaneda and Y. Tabata, *Cancer Sci.*, 2006, **97**, 348.
- (a) H. H. Ahn, J. H. Lee, K. S. Kim, J. Y. Lee, M. S. Kim, G. Khang, I. W. Lee and H. B. Lee, *Biomaterials*, 2008, **29**, 2415; (b) W. T. Godbey, K. K. Wu and A. G. Mikos, *J. Controlled Release*, 1999, **60**, 149; (c) U. Lungwitz, M. Breunig, T. Blunk and A. Gopferich, *Eur. J. Pharm. Biopharm.*, 2005, **60**, 247.
- (a) C. H. Ahn, S. Y. Chae, Y. H. Bae and S. W. Kim, *J. Controlled Release*, 2002, **80**, 273; (b) R. Arote, T. H. Kim, Y. K. Kim, S. K. Hwang, H. L. Jiang, H. H. Song, J. W. Nah, M. H. Cho and C. S. Cho, *Biomaterials*, 2007, **28**, 735.
- Y. X. Sun, X. Zeng, Q. F. Meng, X. Z. Zhang, S. X. Cheng and R. X. Zhuo, *Biomaterials*, 2008, **29**, 4356.
- (a) D. A. Wall and A. L. Hubbard, *J. Cell Biol.*, 1985, **101**, 2104; (b) H. Li and Z. M. Qian, *Med. Res. Rev.*, 2002, **22**, 225; (c) J. M. Bennis, R. I. Mahato and S. W. Kim, *J. Controlled Release*, 2002, **79**, 255; (d) K. Shigeta, S. Kawakami, Y. Higuchi, T. Okuda, H. Yagi, F. Yamashita and M. Hashida, *J. Controlled Release*, 2007, **118**, 262; (e) M. Elfinger, C. Maucksch and C. Rudolph, *Biomaterials*, 2007, **28**, 3448; (f) S. Fumoto, S. Kawakami, Y. Ito, K. Shigeta, F. Yamashita and M. Hashida, *Mol. Ther.*, 2004, **10**, 719.
- (a) O. H. Laitinen, H. R. Nordlund, V. P. Hytonen and M. S. Kulomaa, *Trends Biotechnol.*, 2007, **25**, 269; (b) M. Mamede, T. Saga, T. Ishimori, T. Higashi, N. Sato, H. Kobayashi, M. W. Brechbiel and J. Konishi, *J. Controlled Release*, 2004, **95**, 133; (c) H. Sakahara and T. Saga, *Adv. Drug Delivery Rev.*, 1999, **37**, 89; (d) H. Huang, S. Oizumi, N. Kojima, T. Niino and Y. Sakai, *Biomaterials*, 2007, **28**, 3815; (e) M. S. Kim, K. S. Seo, G. Khang and H. B. Lee, *Langmuir*, 2005, **21**, 4066.
- (a) R. J. DeLange, *J. Biol. Chem.*, 1970, **245**, 907; (b) B. Schechter, R. Silberman, R. Arnon and M. Wilchek, *Eur. J. Biochem.*, 1990, **189**, 327; (c) L. Chen, B. Schechter, R. Arnon and M. Wilchek, *Drug Dev. Res.*, 2000, **50**, 258.
- R. Hernandez-Alcoceba, B. Sangro and J. Prieto, *Annals of Hepatology*, 2007, **6**, 5.
- (a) J. M. Llovet, A. Burroughs and J. Bruix, *Lancet*, 2003, **362**, 1907; (b) A. Follenzi and S. Gupta, *J. Hepatol.*, 2004, **40**, 337; (c) M. J. Willhauck, B. R. Sharif Samani, K. Klutz, N. Cengic, I. Wolf, L. Mohr, M. Geissler, R. Senekowitsch-Schmidtke, B. Goke, J. C. Morris and C. Spitzweg, *Gene Ther.*, 2008, **15**, 214; (d) V. Schmitz, C. Qian, J. Ruiz, B. Sangro, I. Melero and G. Mazzolini, *Gut*, 2002, **50**, 130.
- (a) H. L. Jiang, J. T. Kwon, Y. K. Kim, E. M. Kim, R. Arote, H. J. Jeong, J. W. Nah, Y. J. Choi and T. Akaike, *Gene Ther.*, 2007, **14**, 1389; (b) C. M. Varga, N. C. Tedford, M. Thomas, A. M. Klivanov, L. G. Griffith and D. A. Lauffenburger, *Gene Ther.*, 2005, **12**, 1023; (c) L. Liu, M. A. Zern, M. E. Lizarzaburu, M. H. Nantz and J. Wu, *Gene Ther.*, 2003, **10**, 180.
- J. K. Oh, D. J. Siegwart, H. Lee, G. Sherwood, L. Peteanu, J. O. Hollinger, K. Kataoka and K. Matyjaszewski, *J. Am. Chem. Soc.*, 2007, **129**, 5939.
- E. Emilietri, E. Ranucci and P. Ferruti, *J. Polym. Sci., Part A: Polym. Chem.*, 2005, **43**, 1404.
- J. M. Bennis, J. S. Choi, R. I. Mahato, J. S. Park and S. W. Kim, *Bioconjugate Chem.*, 2000, **11**, 637.